

DESIGN AND ALIGNMENT OF A THREE-MIRROR ANASTIGMAT

by

Emily Mrkvicka

---

Copyright © Emily Mrkvicka 2024

A Master's Report Submitted to the Faculty of the

DEPARTMENT OF OPTICAL SCIENCES

In Partial Fulfillment of the Requirements

For the Degree of

MASTER OF SCIENCES

In the Graduate College

THE UNIVERSITY OF ARIZONA

2024

THE UNIVERSITY OF ARIZONA  
GRADUATE COLLEGE

As members of the Master's Committee, we certify that we have read the report prepared by Emily Mrkvicka, titled Design and Alignment of a Three-Mirror Anastigmat and recommend that it be accepted as fulfilling the dissertation requirement for the Master's Degree.

  
\_\_\_\_\_  
Dr. José Sasián

Date: May 26 2024

  
\_\_\_\_\_  
Dr. Thomas Milster


Date: 5/1/2024

  
\_\_\_\_\_  
Dr. Ronald Driggers

Date: 26 May 2024

Final approval and acceptance of this report is contingent upon the candidate's submission of the final copies of the report to the Graduate College.

I hereby certify that I have read this report prepared under my direction and recommend that it be accepted as fulfilling the Master's requirement.

  
\_\_\_\_\_  
Dr. José Sasián  
Master's Report Committee Chair  
College of Optical Sciences

Date: May 26 2024



ARIZONA

## **ACKNOWLEDGEMENTS**

First, I would like to thank José Sasián, Thomas Milster, and Ronald Driggers for their academic support. Their guidance and service on my defense committee have made this Master's Report possible.

Next, thank you to Albert Ciullo, Sarah Temple, and James Contreras for their professional support. You all have given me the mentorship and opportunities without which I would not have a career in optical engineering.

And finally, thank you to my parents Mark Mrkvicka and Deanna Moody and my husband Ethan Gorham for their emotional support. I was able to pursue this graduate degree because of your never-ending patience.

# Contents

Abstract .....	6
1. Introduction .....	7
1.1 What is a three-mirror anastigmat? .....	7
1.2 History .....	8
1.3 Applications and Examples .....	9
2. Aberration Theory .....	10
3. Design Parameters .....	12
3.1 Advantages .....	12
3.2 Disadvantages .....	14
3.3 TMA Design Space .....	15
4. Manufacturing .....	16
4.1 Materials .....	16
4.1.1 Substrates .....	16
4.1.2 Coatings .....	18
4.2 Manufacturing Methods .....	19
4.2.1 Diamond Turning .....	19
4.2.2 Polishing .....	20
5. Alignment Approach .....	21
5.1 CMM .....	22
5.2 Laser Tracker .....	22
5.3 Theodolite .....	23
5.4 Interferometer .....	24
5.5 Alignment Tools Applied to a TMA .....	25
6. Case Study .....	26
6.1 Design Requirements .....	26
6.2 Optimization .....	26
6.3 Lens Prescription .....	29
6.4 Imaging Performance .....	31
7. Conclusions .....	35
Appendix – Table of Acronyms .....	35
References .....	36

## List of Figures

Figure 1: Layout of a TMA from “Field Guide to Lens Design” by J. Bentley and Craig Olsen .....	7
Figure 2: A timeline of reflective anastigmat design history up to the invention of the TMA, based on "Reflecting anastigmatic optical systems: a retrospective" by A. Rakich.....	8
Figure 3: Ralph optical layout from “Ralph: A Visible/Infrared Imager for the New Horizons Pluto/Kuiper Belt Mission”, Reuter et al.....	9
Figure 4: Optical layout of JWST from JWST User Documentation .....	10
Figure 5: Cassegrain obscuration, courtesy of L. Carlino's article "GSO 8-Inch True Cassegrain" .....	13
Figure 6: TMA with Lyot stop from "Optical Systems Design" by R. Fischer, B. Tadic-Galeb, P.R. Yoder .....	14
Figure 7: Reflective design space from "Field Guide to Lens Design", J. Bentley, C. Olson .....	16
Figure 8: Light-weighted Zerodur mirror substrate, Schott.....	17
Figure 9: Typical optical coatings, Wikipedia.....	18
Figure 10: Diamond turning machine, image from Coherent Corp. ....	20
Figure 11: CNC optical polishing machine, Satisloh.....	21
Figure 12: CMM components, courtesy of Keyence Corp. ....	22
Figure 13: FARO laser tracker with an SMR.....	23
Figure 14: TM6100A theodolite from Leica Geosystems.....	24
Figure 15: Alignment cubes from precision optical.....	24
Figure 16: Various aberrations as presented in interferometric fringe patterns, courtesy of E. Goodwin and J. Wyant.....	25
Figure 17: OSLO operands for case study optimization.....	28
Figure 18: Case study field points for optimization.....	28
Figure 19: Case study lens layout .....	29
Figure 20: Case study lens prescription .....	29
Figure 21: Case study spot size.....	31
Figure 22: Case study MTF .....	32
Figure 23: Case study ray aberration curves.....	33
Figure 24: Case study distortion grid.....	34
Figure 25: Case study wavefront error.....	34

## List of Tables

Table 1: Aberrations of a plane symmetric system from "Introduction to Lens Design" by J. Sasián.....	12
Table 2: Mirror Materials .....	17
Table 3: List of Diamond-Turnable Materials from Fabrication of Optics by Diamond Turning by R. Rhorer and C. Evans .....	19
Table 4: TMA case study design requirements .....	26
Table 5: Case study aspheric data .....	30
Table 6: Acronyms .....	35

## List of Equations

Equation 1: Wavefront Aberration Term for Spherical Aberration .....	11
Equation 2: Wavefront Aberration Term for Coma.....	11
Equation 3: Wavefront Aberration Term for Astigmatism .....	11
Equation 4: Relationship between f-number, focal length, and aperture .....	15
Equation 5: Relationship between f-number and numerical aperture .....	15

## Abstract

With the growing demand for high resolution space imaging systems, reflective architectures have become critical in the world of modern optical design. The three-mirror anastigmat (TMA) is a popular type of reflective telescope, as it is corrected for spherical aberration, coma, and astigmatism. It is also able to handle larger fields of view than the two-mirror Cassegrain telescope, its historical predecessor. When designing TMA, the mirror materials (both substrate and coating) as well as the manufacturing methods must be considered. Depending on the materials chosen, mirrors can be polished or diamond-turned. Alignment approaches must also be investigated during development. 3-dimensional characterization tools such as a CMM or laser tracker may be used for coarse mirror positioning, while interferometric data may be used to inform fine alignment. To demonstrate the performance of a TMA for a given set of requirements, a design case study is performed for a 20cm, f/5 telescope.

# 1. Introduction

## 1.1 What is a three-mirror anastigmat?

A three-mirror anastigmat (TMA) is a type of unobscured reflective telescope that consists of three curved mirrors. Traditionally, each mirror in a TMA is an off-axis conic. If the requirements of the telescope are demanding, there may be additional aspheric coefficients added to the mirror prescriptions. The primary and tertiary mirrors are concave, positively powered optics while the secondary is convex and negatively powered.<sup>1</sup> The off-axis nature of the mirrors allows the aperture to be unobscured, unlike on-axis reflective telescopes such as the Cassegrain. The term “anastigmat” in the title of the TMA indicates that the design form is corrected for spherical aberration, coma, and astigmatism.<sup>2</sup> An example of the layout of a TMA is shown in Figure 1.<sup>3</sup> A TMA can be considered as an off-axis extension of a Cassegrain. The tertiary mirror in a TMA works as an eyepiece that corrects the field-dependent astigmatism and therefore allows for larger fields of view than the Cassegrain architecture. As a note, the TMA architecture can be designed for both focal and afocal configurations.

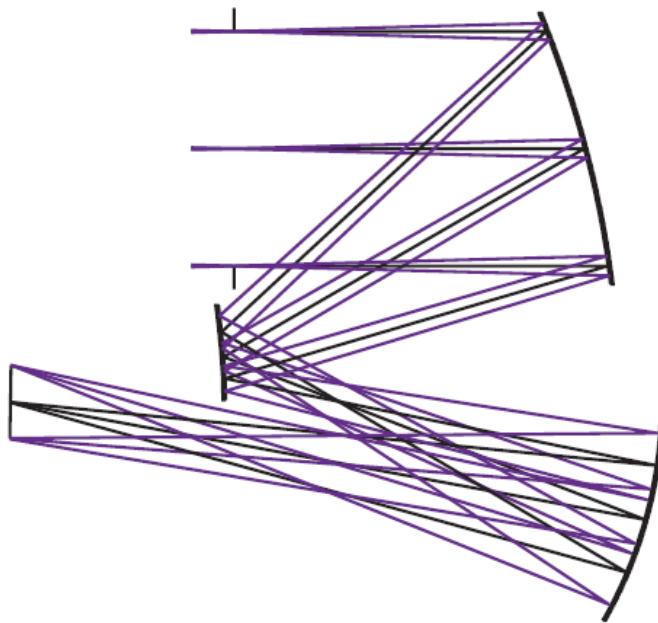


Figure 1: Layout of a TMA from “Field Guide to Lens Design” by J. Bentley and Craig Olsen

## 1.2 History

In the early 1600s, refractive telescopes were the most common forms of imaging systems. While it is widely contested who the first inventor of the telescope was, the Keplerian and Galilean designs are examples of widely recognized refractive telescopes of the time. However, refractive telescopes have a limited range of aperture size. Large aperture sizes pose a couple of issues for lenses. First, quality lenses must have substrates that are free of bubbles and inclusions, which is difficult to accomplish at large diameters. Second, large lenses are heavy and could pose structural issues when considering optomechanical mounting.<sup>4</sup>

One of the most straightforward ways to increase imaging resolution is to increase the system's aperture size, or entrance pupil diameter (EPD). This revelation, combined with the technical difficulties posed by large refractors, led to the advent of reflective telescopes in the mid-1600s. In his paper "Reflecting anastigmatic optical systems: a retrospective," Andrew Rakich characterizes the history of reflective anastigmats by compiling contributions of multiple key historical figures.<sup>5</sup> A brief summary of the history leading up to the development of the three-mirror anastigmat is shown in Figure 2.



Figure 2: A timeline of reflective anastigmat design history up to the invention of the TMA, based on "Reflecting anastigmatic optical systems: a retrospective" by A. Rakich



## 1.3 Applications and Examples

Three-mirror anastigmats have several applications in different fields. One obvious example of the application of reflective telescopes is space and astronomy. Many well-known telescopes of modern times utilize the three-mirror anastigmat architecture. New Horizons, the NASA mission to explore Pluto's surface at close range,<sup>6</sup> uses a three-mirror anastigmat in its Ralph instrument. Ralph's TMA has an entrance pupil diameter (EPD) of 75 millimeters and operates at a f-number of 8.7.<sup>7</sup> The TMA supplies light to two different focal planes in order to characterize the surface of Pluto with two different wavelength spectra. The TMA is a common path for each spectra and the wavelengths are split up with a dichroic element further down the optical train. Figure 3 shows a CAD model of the Ralph instrument on the left and an optical layout on the right. Ralph's mirrors are all off-axis such that the rays all clear the edges of the optics without the need for obscurations or holes in the primary.

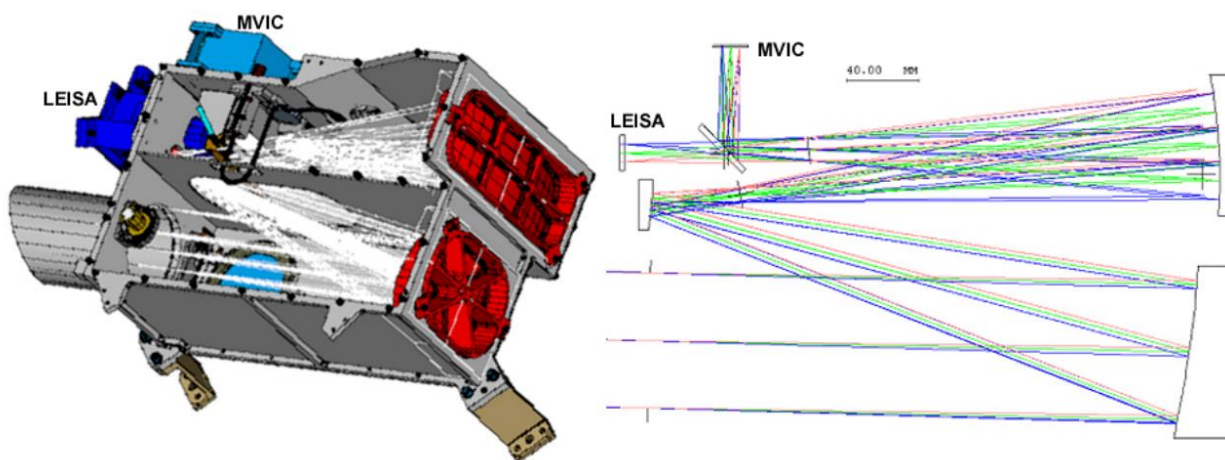


Figure 3: Ralph optical layout from “Ralph: A Visible/Infrared Imager for the New Horizons Pluto/Kuiper Belt Mission”, Reuter et al.

Another well-known example of a TMA used for space science is the James Webb Space Telescope (JWST). JWST is a large-aperture, high-resolution space telescope designed to image faint and distant objects. While JWST also uses a TMA architecture, the optomechanical layout is executed much differently than on Ralph. Figure 4 shows the optical design of JWST.<sup>8</sup> As seen in the layout, the primary

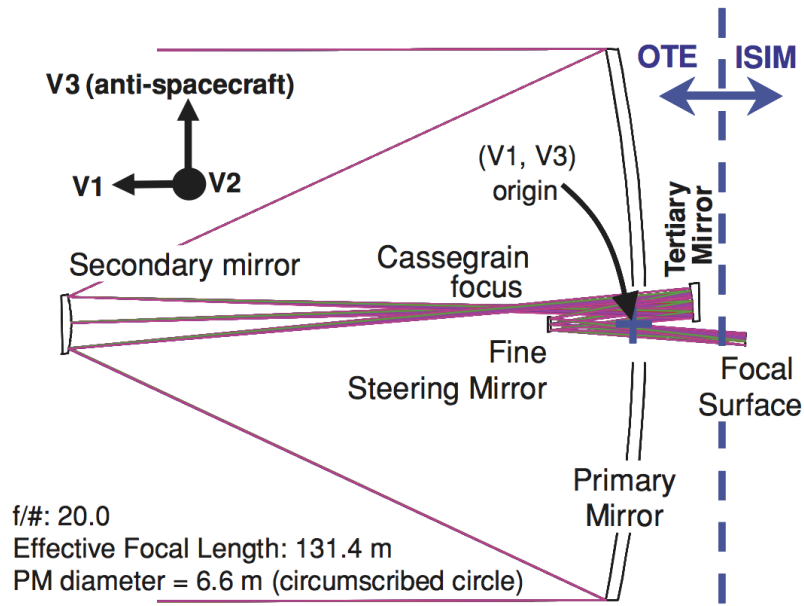


Figure 4: Optical layout of JWST from JWST User Documentation

is not as off-axis as Ralph's primary and requires a hole in the center to allow rays to pass through, reminiscent of a Cassegrain. Although the optomechanical structure of JWST is similar to a Cassegrain, JWST still has a tertiary mirror that corrects aberrations and classifies the telescope as a TMA. JWST is currently the largest space telescope to have ever launched. With an aperture of 6.6 meters, JWST has an EPD that is 88 times the size of Ralph's EPD.

## 2. Aberration Theory

As previously mentioned, an astigmat is an optical design that is corrected for spherical aberration, coma, and astigmatism. Spherical aberration is defined as the variation of focal length with pupil radius. Coma is defined as the variation of magnification with pupil position. Astigmatism is defined as the variation of optical power between the tangential and sagittal planes of the system.<sup>9</sup>

The wavefront aberration function is a mathematical description of the deformation of the wavefront as a result of each aberration in a given system. The term for spherical aberration is written in vector form as:

$$W(\vec{H}, \vec{\rho}) = W_{040}(\vec{\rho} \cdot \vec{\rho})^2$$

*Equation 1: Wavefront Aberration Term for Spherical Aberration*

The term for coma is written as:

$$W(\vec{H}, \vec{\rho}) = W_{131}(\vec{H} \cdot \vec{\rho})(\vec{\rho} \cdot \vec{\rho})$$

*Equation 2: Wavefront Aberration Term for Coma*

The term for astigmatism is written as:

$$W(\vec{H}, \vec{\rho}) = W_{222}(\vec{H} \cdot \vec{\rho})^2$$

*Equation 3: Wavefront Aberration Term for Astigmatism*

For each of the equations above,  $H$  describes the field and  $\rho$  describes the aperture. In systems that are axially symmetric, the coma and astigmatism terms are simplified since the dot product between two parallel vectors is simply equal to the product of their magnitudes. However, TMAs are usually not axially symmetric systems due to their off-axis conics, so the angle between  $\vec{H}$  and  $\vec{\rho}$  is particularly critical.

Although TMAs are not axially symmetric, they are generally plane symmetric which can still help simplify calculations. Table 1 is a table of aberrations in vector form for plane symmetric systems.<sup>10</sup> The aberration forms in the table include a new vector,  $\vec{l}$ , which is a unit vector describing the plane of symmetry. For a TMA, the following aberrations from the table are corrected: uniform astigmatism, uniform coma, and spherical aberration. In the design of a TMA, optical design software such as Zemax, Code V, or OSLO is used to optimize the mirror curvatures and asphere coefficients to correct for these aberrations.

Table 1: Aberrations of a plane symmetric system from "Introduction to Lens Design" by J. Sasián

First group	
$W_{00000}$	Piston
Second group	
$W_{01001}(\vec{i} \cdot \vec{\rho})$	Field displacement
$W_{10010}(\vec{i} \cdot \vec{H})$	Linear Piston
$W_{02000}(\vec{\rho} \cdot \vec{\rho})$	Defocus
$W_{11100}(\vec{H} \cdot \vec{\rho})$	Magnification
$W_{20000}(\vec{H} \cdot \vec{H})$	Quadratic Piston
Third group	
$W_{02002}(\vec{i} \cdot \vec{\rho})^2$	Uniform astigmatism
$W_{11011}(\vec{i} \cdot \vec{H})(\vec{i} \cdot \vec{\rho})$	Anamorphic distortion
$W_{20020}(\vec{i} \cdot \vec{H})^2$	Quadratic piston
$W_{03001}(\vec{i} \cdot \vec{\rho})(\vec{\rho} \cdot \vec{\rho})$	Uniform coma
$W_{12101}(\vec{i} \cdot \vec{\rho})(\vec{H} \cdot \vec{\rho})$	Linear astigmatism
$W_{12010}(\vec{i} \cdot \vec{H})(\vec{\rho} \cdot \vec{\rho})$	Field tilt
$W_{21001}(\vec{i} \cdot \vec{\rho})(\vec{H} \cdot \vec{H})$	Quadratic distortion
$W_{21110}(\vec{i} \cdot \vec{H})(\vec{H} \cdot \vec{\rho})$	Quadratic distortion
$W_{30010}(\vec{i} \cdot \vec{H})(\vec{H} \cdot \vec{H})$	Cubic piston
$W_{04000}(\vec{\rho} \cdot \vec{\rho})^2$	Spherical aberration
$W_{13100}(\vec{H} \cdot \vec{\rho})(\vec{\rho} \cdot \vec{\rho})$	Linear coma
$W_{22200}(\vec{H} \cdot \vec{\rho})^2$	Quadratic astigmatism
$W_{22000}(\vec{H} \cdot \vec{H})(\vec{\rho} \cdot \vec{\rho})$	Field curvature
$W_{31100}(\vec{H} \cdot \vec{H})(\vec{H} \cdot \vec{\rho})$	Cubic distortion
$W_{40000}(\vec{H} \cdot \vec{H})^2$	Quartic piston

## 3. Design Parameters

### 3.1 Advantages

One of the major advantages of the TMA architecture is the ability to use off-axis aspheres to avoid needing an obscuration. Telescopes such as Cassegrains and Ritchey Chretien's have secondary mirrors that block part of the aperture of the primary mirror with both the mirror itself and the "spider" structure used to hold the secondary mirror in place. The structure that blocks the primary can cause

unwanted diffraction effects in the imaging system. The obscuration formed by the on-axis secondary causes a decrease in overall transmission and negatively impacts the resolution of the system. Figure 5 shows an example of a Cassegrain obscuration.<sup>11</sup> The TMA architecture does not see these negative impacts since an obscuration is not necessary.



*Figure 5: Cassegrain obscuration, courtesy of L. Carlino's article "GSO 8-Inch True Cassegrain"*

Another advantage of the TMA is that it can support a larger range of fields of view than two mirror systems. This is because the tertiary mirror corrects for field-dependent astigmatism. While there are variations on how a TMA can be structured, in general the primary and secondary create an intermediate image that is then corrected by the tertiary mirror.

A third advantage of TMAs is that the design has an opportunity for stray light mitigation. When designing imaging systems for space applications, the extreme brightness of the sun in comparison to the actual target of the imaging system can make stray light an especially critical issue. When light is scattered at the entrance aperture, it can cause unwanted effects that degrade imaging performance.

However, if a TMA is designed with an accessible exit pupil, a Lyot stop can be used at the pupil plane to block stray light.<sup>12</sup> Figure 6 demonstrates this principle.

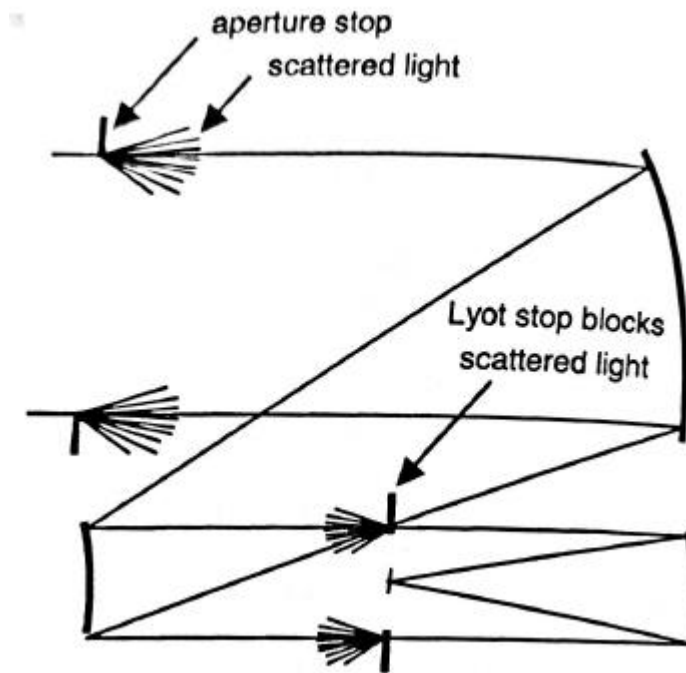


Figure 6: TMA with Lyot stop from "Optical Systems Design" by R. Fischer, B. Tadic-Galeb, P.R. Yoder

## 3.2 Disadvantages

One of the disadvantages of TMAs is the added manufacturing cost and schedule. TMAs always include conical mirrors and sometimes involve more aspheric coefficients, depending on the design. If high imaging performance is needed for large fields of view, the shape of the mirrors can become more complex. In general, mirrors take longer to manufacture and are more expensive than lenses. The cost and schedule are only increased when off-axis aspheres are introduced.

The alignment of a TMA is also more complex than an on-axis system. An on-axis two-mirror system such as a Cassegrain can be aligned simply by using an interferometric return as feedback while iteratively decentering the secondary mirror relative to the primary mirror until the fringes are nulled.

However, an off-axis TMA has optics without a common optical axis. This makes the alignment process less straight forward and potentially more expensive and time consuming.

Another downside of the TMA architecture is that the addition of more mirrors adds surface figure error to the imaging error budget. Even if mirrors are manufactured to the limits of polishing technology, systems with large mirrors can still have their error budgets dominated by surface figure error. Adding another mirror to a system adds another significant surface figure error to account for.

### 3.3 TMA Design Space

Figure 7 shows the design space for common reflective architectures.<sup>3</sup> The y-axis shows the half-field of view (HFOV) in angle space. The x-axis shows the numerical aperture and f-number. The f-number and numerical aperture both describe the relationship between the focal length and the entrance pupil diameter of the system. The relationship is written in Equation 4.

$$f/\# = \frac{f}{D}$$

*Equation 4: Relationship between f-number, focal length, and aperture*

where  $f$  is the effective focal length of the system and  $D$  is the entrance pupil diameter.<sup>9</sup> Equation 5 describes the relationship between f-number and numerical aperture.

$$f/\# = \frac{1}{2NA}$$

*Equation 5: Relationship between f-number and numerical aperture*

where  $NA$  is the numerical aperture.

The design space graphic is a useful tool that helps select a reflective architecture depending on the requirements needed for the application. The appropriate design space for the TMA architecture is roughly defined here is a HFOV between 1.5 and 5.5 degrees with an f-number between 2.5 and 10 (or a numerical aperture between 0.05 and 2).

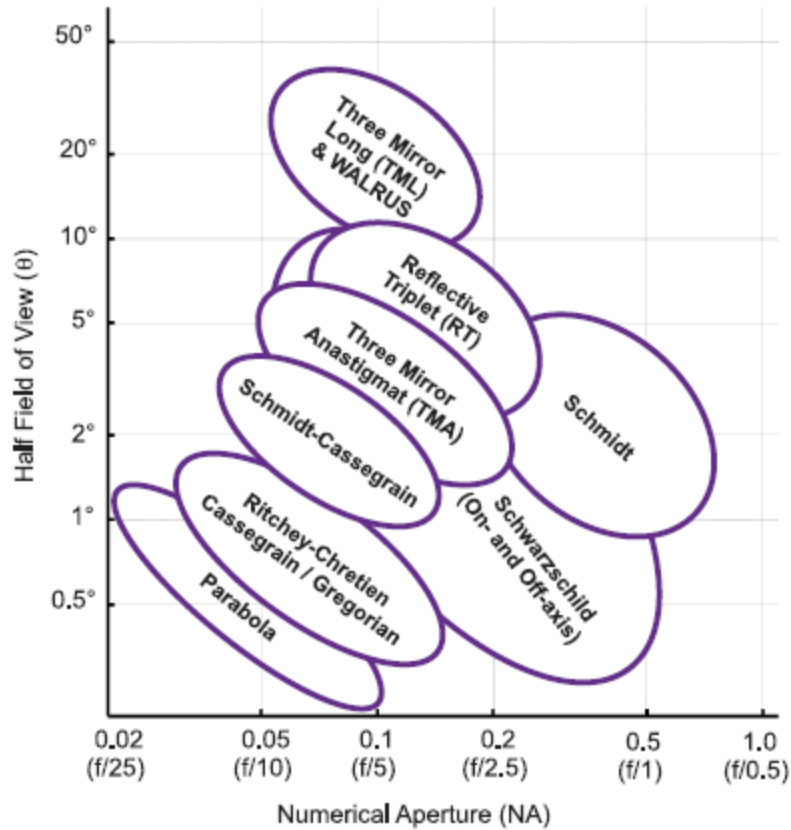


Figure 7: Reflective design space from "Field Guide to Lens Design", J. Bentley, C. Olson

## 4. Manufacturing

### 4.1 Materials

#### 4.1.1 Substrates

Mirrors for reflective systems can be manufactured with either glass or metal. Metal mirrors are typically polished from aluminum. Glass mirrors are created from highly polished glass substrates that are then coated with a reflective coating. In refractive design, the choice of lens substrate is highly dependent on wavelength spectra as the material will help to combat chromatic aberrations. However, chromatic aberrations are not present in reflective design, so material choice depends on other factors. Mass, thermal expansion, manufacturability, and cost are a few of the factors in mirror material selection. Table 2 shows



a list of popular mirror materials with their corresponding coefficients of thermal expansion (CTE) and their densities.

*Table 2: Mirror Materials*

Material	CTE [ $10^{-6}$ /K]	Density [g/cm <sup>3</sup> ]
Zerodur <sup>13</sup>	0.00	2.53
Fused silica <sup>14</sup>	0.50	2.20
Borofloat (borosilicate) <sup>15,16</sup>	3.25	2.23
N-BK7 <sup>17</sup>	2.40	2.51
Soda-lime glass (float glass) <sup>18</sup>	8.60	2.48
Aluminum <sup>19</sup>	23.2	2.7

Mass becomes an issue especially with space telescopes with large apertures. Many mirror materials can be lightweighted by machining out unnecessary material from the back of the mirror while leaving a supporting structure behind. Figure 8 shows an example of a Zerodur mirror substrate from Schott that has been lightweighted by removing triangular wedges of the glass.<sup>13</sup>

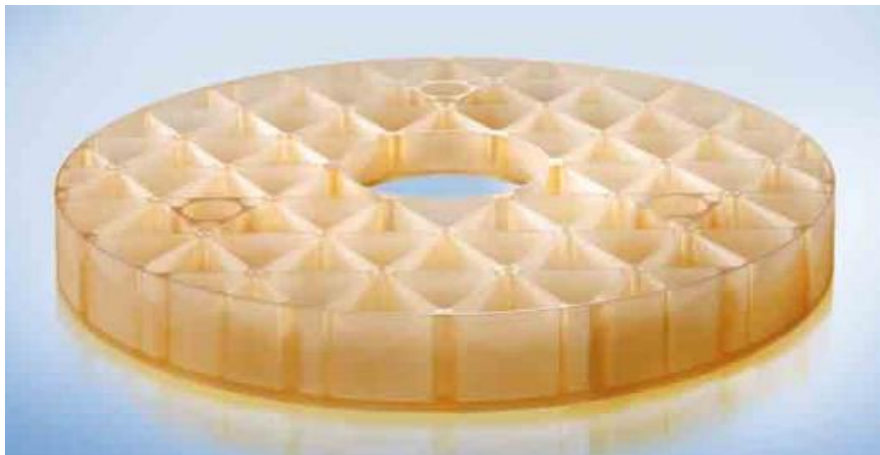


*Figure 8: Light-weighted Zerodur mirror substrate, Schott*

Thermal expansion is an issue for optical systems as it can cause optics to become misaligned or stressed as a result of the changing temperature in the operating environment of the system. One solution to this issue is to use a material with a low coefficient of expansion. For example, Zerodur from Schott has an extremely low CTE and therefore has negligible shift with temperature. Another solution to the thermal issue is to use aluminum mirrors with a housing that is also aluminum. Although aluminum has a CTE that is much higher than any of the other glass, quartz or ceramic materials listed in Table 1, matching the CTE of the mirrors and the housing will allow the thermal shift between the two to be the same. If the thermal shift between the housing and optics are the same, this results in no misalignment of the optics. This method was used on the Ralph instrument on the New Horizons mission. Ralph's entire TMA was constructed from a single block of grain-aligned 6061-T6 aluminum which desensitizes the system from thermal shift.<sup>20</sup>

#### 4.1.2 Coatings

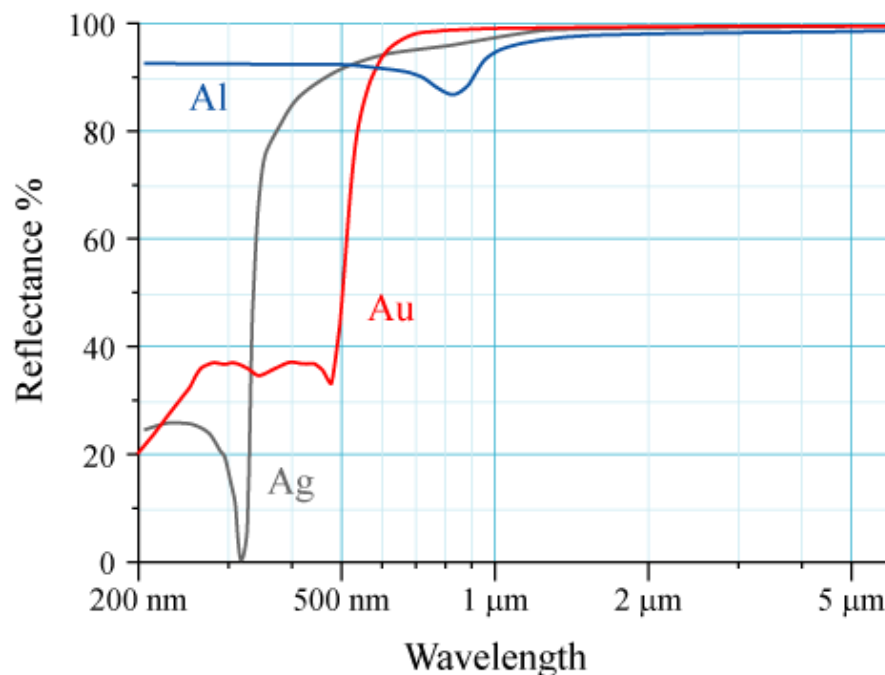


Figure 9: Typical optical coatings, Wikipedia

For mirrors that are made with glass substrates, coatings must be applied to achieve proper reflectivity in the desired wavelength ranges. For specialty projects, custom coatings may be designed

depending on the application. In general, mirror coatings are typically aluminum, silver, or gold. While each coating varies on the specific design, Figure 9 shows reflectance curves for typical mirror coatings.<sup>21</sup> It is common for gold coatings to be used for IR telescopes while silver and aluminum are used for visible systems.

## 4.2 Manufacturing Methods

Different methods of shaping aspheric mirrors may be used depending on the substrate material and the level of precision required by the application. Understanding the manufacturing methods are a key part of the design and tolerance process as the surface figure is often the dominant factor in a telescope's error budget. The two methods discussed here are diamond turning and polishing.

### 4.2.1 Diamond Turning

Diamond turning is a mirror manufacturing method that can be used for metal, crystal, and plastic.<sup>22</sup> Table 3 gives a full list of the materials that are able to be diamond turned. Diamond turning can be a faster and cheaper alternative to polishing. This method is accomplished with a single point diamond on a lathe. Figure 10 shows an example of a diamond turning machine used at Coherent Corp.<sup>23</sup>

The disadvantage of diamond turning is that it will always leave a ring pattern behind as the part is shaped. The periodic shape of the surface roughness is limited by the resolution of the cutting tool. Currently, the maximum abilities of diamond cutting are not comparable to the abilities of polishing methods. However, telescopes that perform at longer wavelengths are less sensitive to surface roughness and are favorable applications for the diamond turning method.

*Table 3: List of Diamond-Turnable Materials from Fabrication of Optics by Diamond Turning by R. Rhorer and C. Evans*

Metals	Nonmetals	Plastics
Aluminum	Calcium fluoride	Polymethylmethacrylate
Brass	Magnesium fluoride	Polycarbonates
Copper	Cadmium telluride	Polyimide
Beryllium copper	Zinc selenide	
Bronze	Zinc sulphide	

Gold	Gallium arsenide
Silver	Sodium chloride
Lead	Calcium chloride
Platinum	Germanium
Tin	Strontium fluoride
Zinc	Sodium fluoride
Electroless nickel	KPD
	KTP
	Silicon

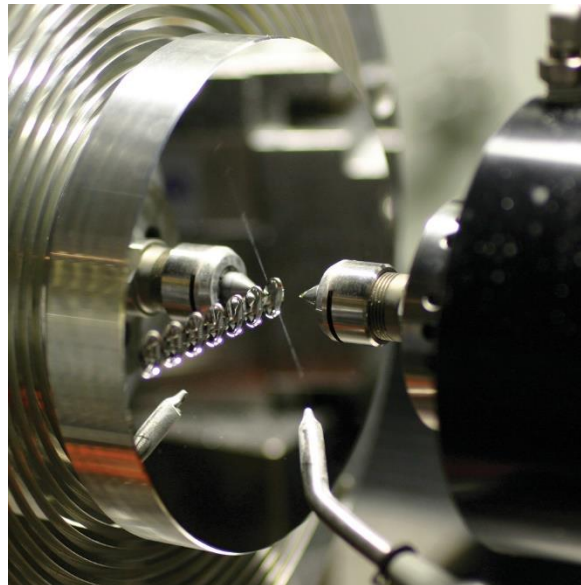


*Figure 10: Diamond turning machine, image from Coherent Corp.*

### 4.2.2 Polishing

Polishing optics is the process of iteratively removing material from a substrate with a range of abrasive materials until the desired shape and roughness are achieved.<sup>24</sup> This is the process that is typically used for glass and quartz substrates that cannot be diamond turned. The surface roughness leftover from polishing methods has the ability to be lower in peak-to valley values than diamond turning. The pattern of the roughness is also random in comparison to the periodic pattern left by a diamond

turning machine. A random distribution of surface roughness is often preferable, as a periodic pattern could cause unwanted diffraction effects. The disadvantage of the polishing method is that cost and schedule can both be impacted. Figure 11 shows an example of a CNC polishing machine from Satisloh.<sup>25</sup>



*Figure 11: CNC optical polishing machine, Satisloh*

## 5. Alignment Approach

After a telescope is designed and materials are selected, an alignment plan must be developed. It is important to understand what metrology tools will be used to align an optical system as the alignment tolerances are a key piece of the overall error budget. There are multiple approaches available for telescope alignment, many of which use multiple metrology tools at different stages. This section will cover four tools commonly used for optical alignment: a CMM, a laser tracker, a theodolite, and an interferometer.

## 5.1 CMM

A coordinate measuring machine (CMM) is one of the common tools used for characterization and alignment of optics. A CMM uses a probe that characterizes hardware by feeding three-dimensional data to encoders.<sup>26</sup> A CMM is useful for optical alignment as it can characterize the optical surface of a mirror and its position relative to other datums, such as the flat back surface of the mirror, or the mirror edges that may be used for bonding. For optical alignment, it is useful to know precisely how the optical surfaces relate physically to their mechanical interfaces. Figure 12 is a diagram of the common components of a CMM from Keyence Corp.<sup>27</sup> The accuracy of a CMM depends on the make and model but is generally between 10-20 microns.

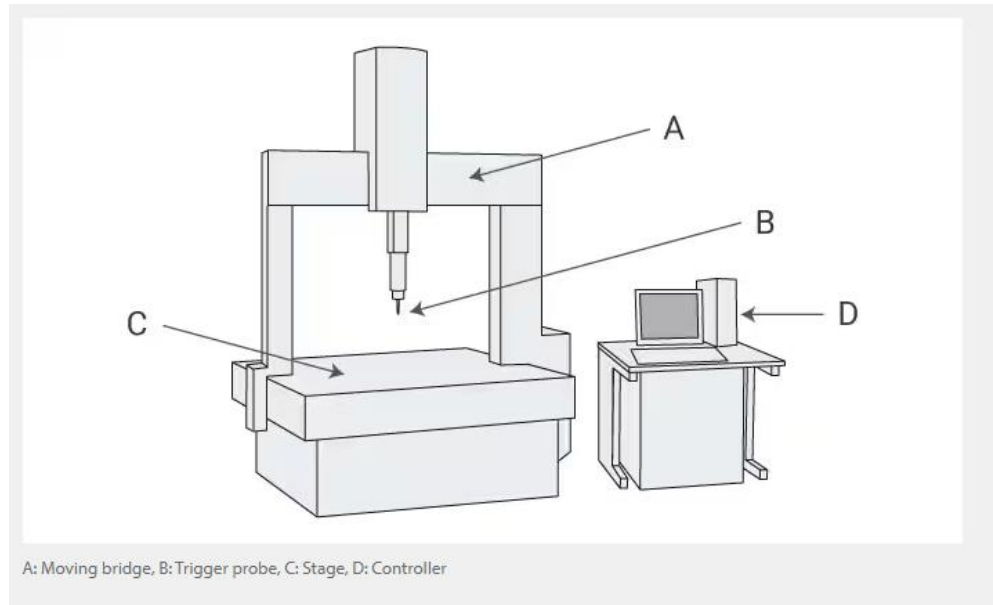


Figure 12: CMM components, courtesy of Keyence Corp.

## 5.2 Laser Tracker

Another tool commonly used in optical alignment is a laser tracker. A laser tracker is similar to a CMM in that it tracks 3-dimensional cartesian data. A laser tracker uses a spherically mounted retroreflector (SMR) which contains a corner cube that reflects the laser back to the tracker and reports a coordinate for the point in space occupied by the SMR. Figure 13 shows an example of a laser tracker

from FARO tracking an SMR.<sup>28</sup> SMRs are generally magnetic and can be placed in kinematic “nests” such that they always mount to the same location after being moved to multiple points. Optical benches for telescopes can be quickly characterized multiple times with high repeatability if kinematic SMR mounts are used. It is important to note that only rigid bodies should be measured with laser trackers and CMMs since they require physical contact for measurement. The physical contact required could cause a flexible surface to shift and give unreliable results.



*Figure 13: FARO laser tracker with an SMR*

## 5.3 Theodolite

A theodolite is a different type of alignment tool in that it measures angles rather than 3-dimensional coordinates. While a laser tracker can use 3-dimensional coordinates to calculate angles, a theodolite can measure angular quantities with higher precision. Theodolites include a refractive telescope that sends a collimated beam to a reflective target. The beam that returns can be viewed through the telescope’s eyepiece. Knobs on the theodolite are then used to align the theodolite’s reticle to the returning beam. When the return is aligned, the display reads out angles in both the horizontal and vertical axes.<sup>26</sup> Figure 14 shows an example of a theodolite from Leica Geosystems.<sup>29</sup> Theodolites are useful for telescope alignment when referencing the telescope’s optical axis or boresight angle to the coordinate system of the optical bench. Reflective references such as alignment cubes can be mounted to the optical bench for this purpose. Figure 15 shows examples of alignment cubes from Precision Optical.<sup>30</sup>



*Figure 14: TM6100A theodolite from Leica Geosystems*

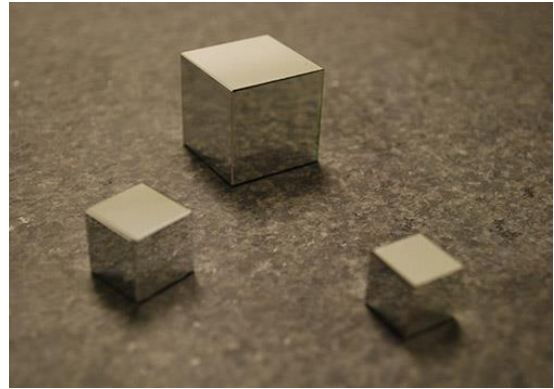


*Figure 15: Alignment cubes from precision optical*

## 5.4 Interferometer

The most precise alignment tool discussed here is an interferometer. An interferometer measures errors using the interference between two beams of light. Interferometers vary in design, but in general interferometers are optical instruments that split a beam into two beams. One beam interacts with the unit under test (UUT) before returning to the interferometer and interfering with the other unaffected beam. The interference pattern between the two beams at the detecting surface of the interferometer can be interpreted to determine the errors of the UUT. An interferometer can be used to test individual optical surface errors or system alignment errors. Figure 16 shows examples of interferometric patterns resulting from combinations of spherical aberration, coma, and astigmatism.<sup>31</sup>



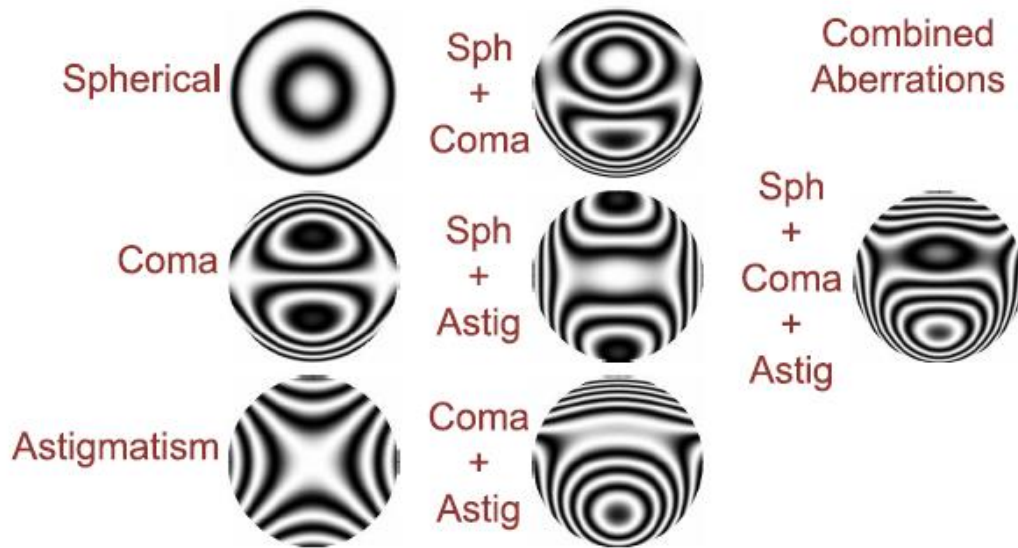


Figure 16: Various aberrations as presented in interferometric fringe patterns, courtesy of E. Goodwin and J. Wyant

## 5.5 Alignment Tools Applied to a TMA

When aligning a TMA, a combination of the previously discussed tools may be necessary depending on the complexity of the design. The less precise tools (CMM, laser tracker) can be used as a coarse measure to get the system roughly aligned while the more precise tools can be used to achieve optimized alignment (interferometer). In the paper “TMA Optical Alignment Using Code V Automatic Design, Code V Alignment Optimization, and Zernike Sensitivity Analysis”, Staples, Brown, and Primeau discuss a method of aligning a TMA in which interferometric measurements are fed to a Code V model that is then optimized for the best alignment.<sup>32</sup>

## 6. Case Study

### 6.1 Design Requirements

To demonstrate the design and optimization of a TMA, some arbitrary requirements were generated that fall roughly within the trade space outlined in Figure 7. The first order requirements used for the design study are shown in Table 4.

*Table 4: TMA case study design requirements*

Specification	Requirement
Aperture Diameter	20 cm
HFOV	1.5°
Distortion	1%
F-number	5
RMS Wavefront Error	100nm

### 6.2 Optimization

The lens design for this case study was completed in the lens design software OSLO. Figure 17 shows the user defined optimization that was used for the design. Note that this figure does not include the operands for image performance; further operands were generated to optimize performance based on wavefront error (WFE).

Optimization operands in OSLO are written with the following inputs in order: field point, ray, wavelength, and surface. Figure 18 shows the numbered field points as they have been defined. Only one side of the field has field points that have been defined for optimization since the TMA is a plane-symmetric system. It can be assumed that the field points across the plane of symmetry would have identical performance regardless of whether they are defined in the optimization or not.

Operands 1 through 4 in Figure 17 relate to the image surface. The first two operands control the centration and tilt of the image surface and ensure the chief ray is incident in the center of the surface at a normal angle. Operands 3 and 4 control the focal length of the telescope. Since the TMA is off-axis, paraxial focal length operands cannot be used effectively. Instead, the image height is held to the appropriate size that corresponds to the aperture and f-number of the system.

Operands 5 through 9 set a dummy surface to be placed at the intermediate image formed by the primary and secondary mirror. Having a surface set up at this location becomes useful when creating clearance between the intermediate image and the other rays. An accessible intermediate image allows for a physical field stop to be placed at the image location to help mitigate stray light.

Operands 10 through 14 set a dummy surface to be set at the exit pupil. Similar to the intermediate image, it is useful for the exit pupil to be physically accessible so that a Lyot stop may be placed there as demonstrated in Figure 6.

Operands 15 and 16 limit the size of the tertiary mirror in order to keep the telescope volume under control. Optical design optimizers must have limits set to keep the design within reasonable manufacturing limitations.

Operands 16 through 21 are clearance operands. The optimizer must have explicit limitations that are set to allow rays to pass from one mirror to another with no obscurations. These operands determine how off-axis the aspheric mirrors must be.

Operands 22 and 23 help to keep distortion under control, as they hold the chief ray heights to be equal in the X and Y axes between various field points.

OP	MODE	WGT	NAME	DEFINITION
1	Min	1.000000	imgsurf	$Y(1,1)$
2	Min	1.000000		$YA(1,1)$
3	Min	1.000000		$Y(2,1)+26.2$
4	Min	1.000000		$Y(3,1)-26.2$
5	Min	1.000000	intimg	$Y(1,2,1,5)-Y(1,3,1,5)$
6	Min	1.000000		$Y(1,1,1,5)$
7	Min	1.000000		$YA(1,1,1,5)$
8	Min	1.000000		$Y(2,2,1,5)-Y(2,3,1,5)$
9	Min	1.000000		$Y(3,2,1,5)-Y(3,3,1,5)$
10	Min	1.000000	exitpupil	$Y(2,1,1,8)-Y(3,1,1,8)$
11	Min	1.000000		$Y(1,1,1,8)$
12	Min	1.000000		$Y(2,2,1,8)-Y(3,2,1,8)$
13	Min	1.000000		$Y(2,3,1,8)-Y(3,3,1,8)$
14	Min	0.000000	m3 size	$Y(1,3,1,6)-Y(1,2,1,6)$
15	Min	1.000000		$O14 < 400.0$
16	Min	1.000000	m2clr1	$ZG(3,3,1,2)-ZG(2,2,1,4)$
17	Min	0.000000		$YG(3,3,1,2)-YG(2,2,1,4)$
18	Min	1.000000		$O17 > 20.0$
19	Min	1.000000	intimgclr	$ZG(3,2,1,5)-ZG(2,3,1,7)$
20	Min	0.000000		$YG(3,2,1,5)-YG(2,3,1,7)$
21	Min	1.000000		$O20 > 10.0$
22	Min	1.000000	distortion	$X(5,1)-X(6,1)$
23	Min	1.000000		$Y(5,1)-Y(2,1)$

Figure 17: OSLO operands for case study optimization

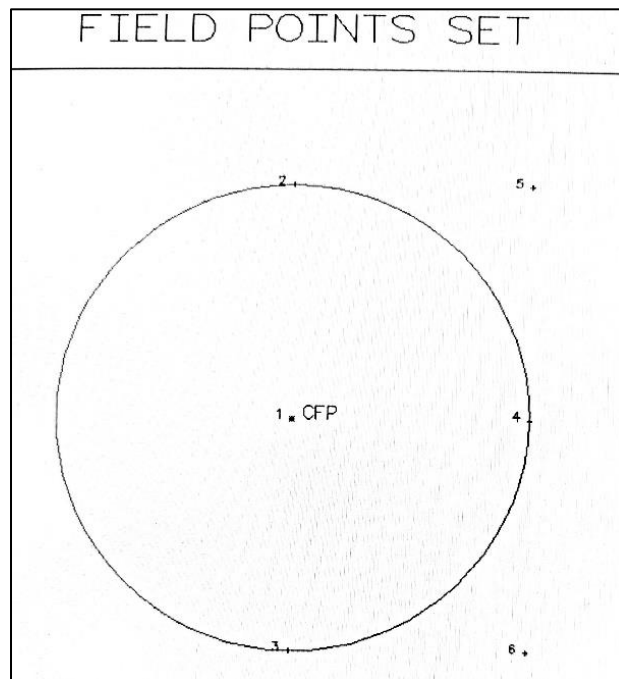


Figure 18: Case study field points for optimization

## 6.3 Lens Prescription

Figure 19 shows the lens layout of the TMA that results from the optimization. The intermediate image plane and exit pupil plane are indicated by flat dummy surfaces that indicate where the field stop and Lyot stop would be located, respectively. Figure 20 shows the lens prescription of the system as viewed from the OSLO design interface.

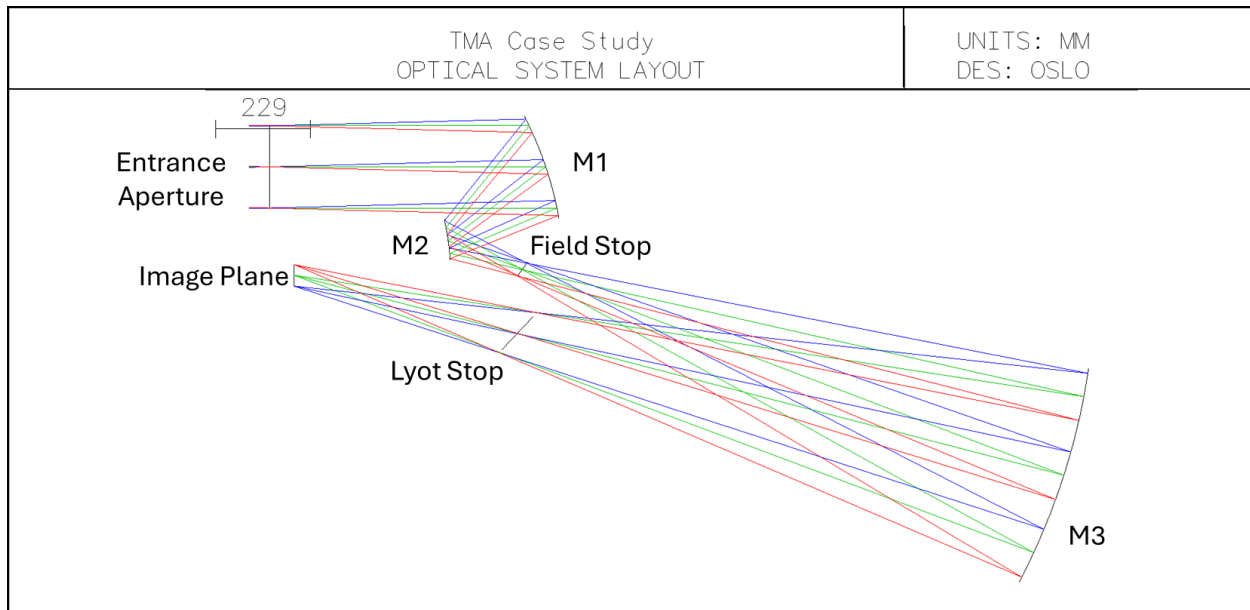


Figure 19: Case study lens layout

Ent beam radius		100.000000	Field angle		1.500000	Primary wavln		1.000000
SRF	RADIUS	THICKNESS	APERTURE	RADIUS	GLASS	SPECIAL		
OBJ	0.000000	1.0000e+20	2.6186e+18	AIR				
AST	0.000000	425.073692	100.000000	AS	AIR	F		
2	0.000000	288.435979	111.130946	S	AIR			
3	-771.460815	-274.041162	118.683908	SX	REFLECT	CA		
4	-496.767711	174.761961	41.541256	SX	REFLECT	CA		
5	0.000000	1.3915e+03	21.573995	S	AIR	FC		
6	-1.6037e+03	-1.4040e+03	251.607986	SX	REFLECT	CA		
7	0.000000	-542.953423	57.224129	S	AIR	FC		
8	0.000000	0.000000	26.214538	S	AIR	C		
IMS	0.000000	0.000000	26.214538	S		F		

Figure 20: Case study lens prescription

Table 5 lists the aspheric information for each of the mirrors. Due to the requirement that the intermediate image and exit pupil be physically accessible, aspheric coefficients had to be added to the mirrors to compensate for the performance loss.

*Table 5: Case study aspheric data*

Mirror	Conic Constant	4 <sup>th</sup> Order Coefficient	6 <sup>th</sup> Order Coefficient	Decenter
Primary	-0.6095	3.5514e-11	1.6794e-17	-255.85mm
Secondary	-6.5469	3.9318e-10	-3.0552e-15	0.75mm
Tertiary	-0.1162	-1.3978e-13	2.9864e-20	7.22mm

## 6.4 Imaging Performance

This section will analyze the imaging performance of the case study design using several different metrics.

Figure 21 shows the spot diagrams that correspond to the field points from Figure 18. Note that the black circle represents the size of the airy disk. The spot size is smaller than the airy disk for most field points which indicates that the design is near diffraction-limited.

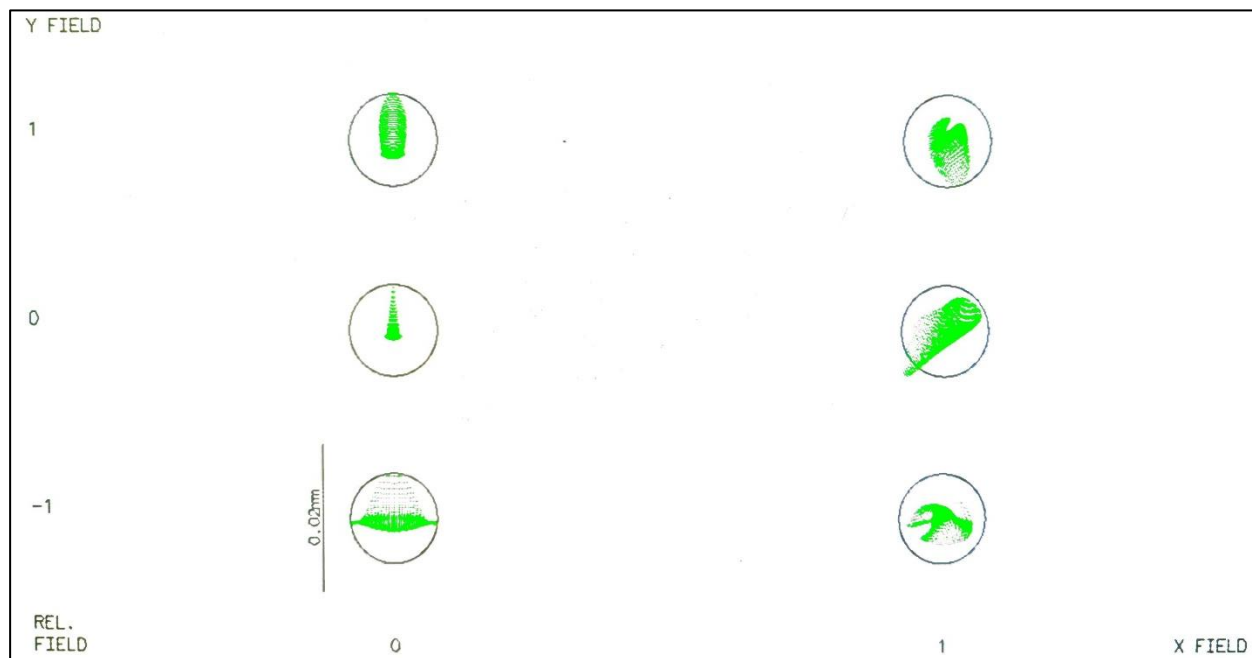


Figure 21: Case study spot size

Figure 22 shows the system modulation transfer function (MTF) out to 100 cycles per millimeter. The green line with circle markers indicates the diffraction limit while the blue lines indicate the actual system MTF for the tangential and sagittal planes. The MTF again indicates the case study design is near diffraction-limited.

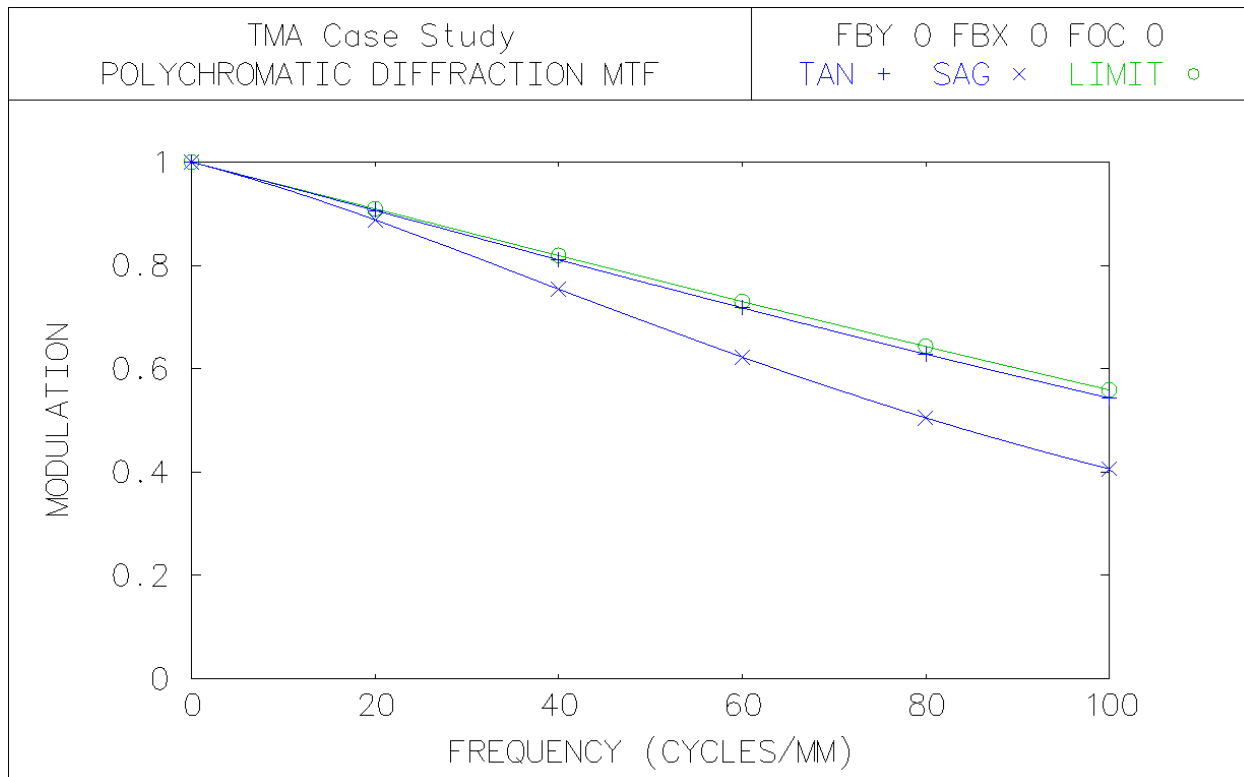


Figure 22: Case study MTF



Figure 23 shows the OSLO ray intercept curve analysis which includes ray aberration, astigmatism, spherical aberration, and distortion curves. Chromatic aberration curves would also be shown here if the system were not monochromatic. Note that only one wavelength was defined for the system as the system is all reflective and unaffected by chromatic aberrations.

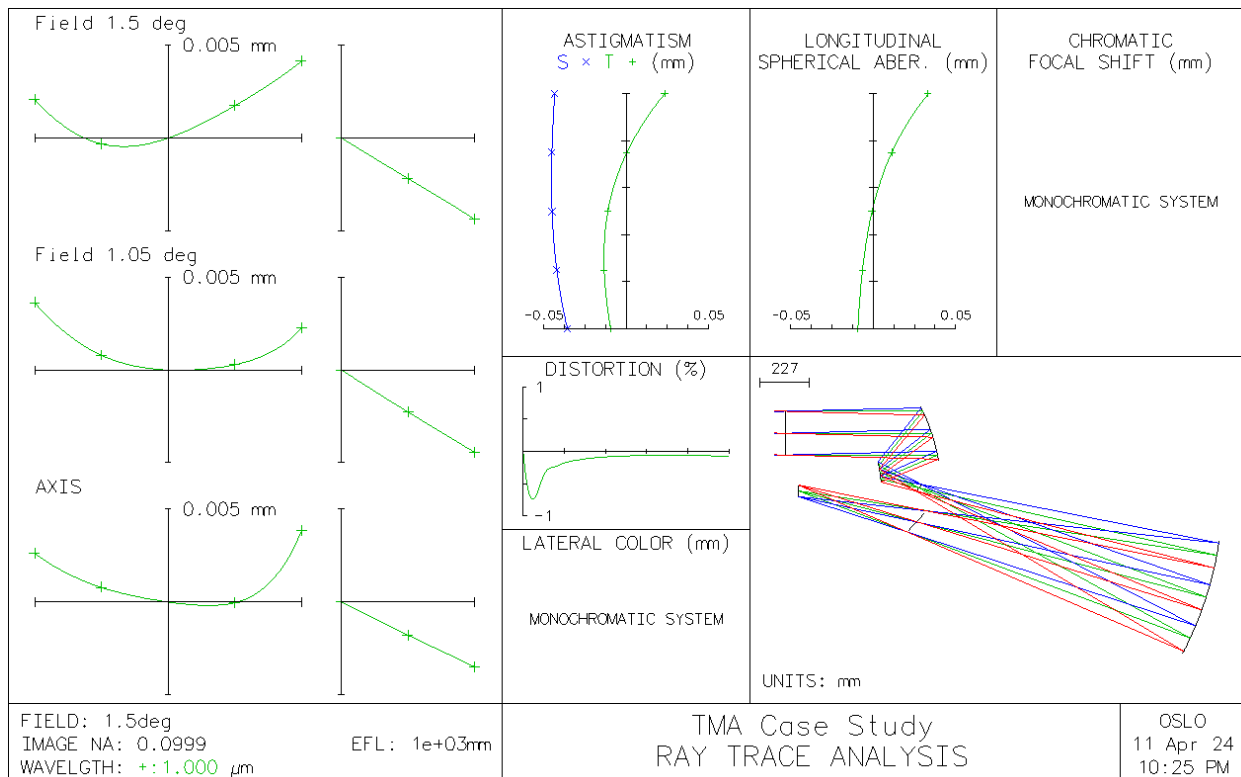


Figure 23: Case study ray aberration curves

Figure 24 shows the full distortion grid for the system. The curves in this graphic indicate that the design meets the 1% requirement.

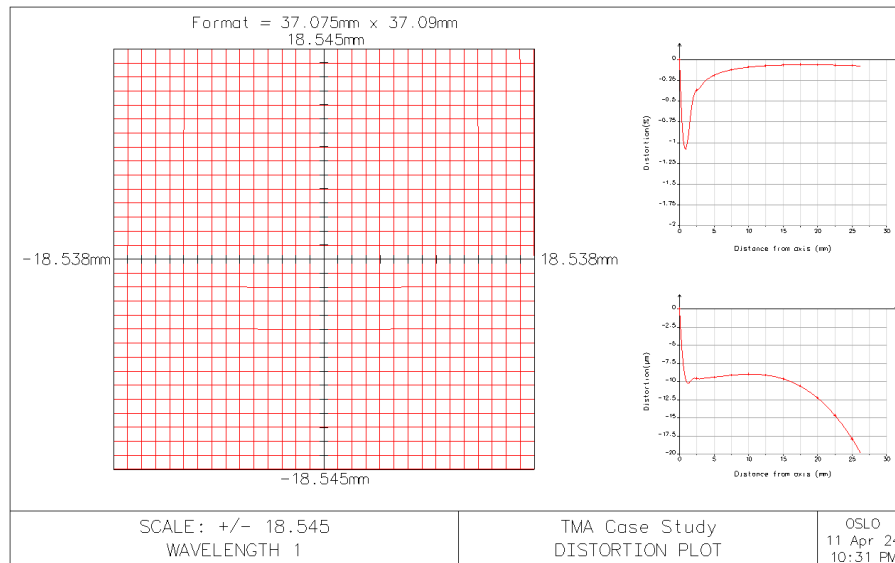


Figure 24: Case study distortion grid

Figure 25 shows the wavefront plots for field points that are on-axis, at 70% of the field, and 100% of the field. Wavefront here is listed in waves. The system wavefront is 1000 nanometers, so the maximum RMS wavefront error is about 68 nanometers.

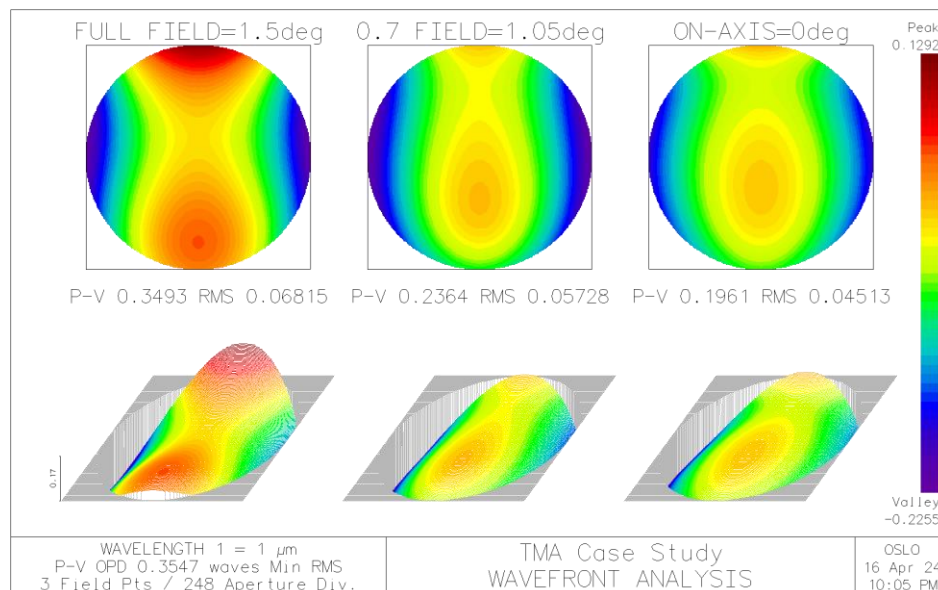


Figure 25: Case study wavefront error

## 7. Conclusions

The three-mirror anastigmat is a telescope architecture that can improve optical performance at larger fields of view than a Cassegrain because its tertiary mirror acts as an eyepiece that corrects field-dependent astigmatism. The TMA architecture is especially effective for half fields of view between 1.5 and 5.5 degrees and f-numbers between 2.5 and 10. When designing a TMA, the impacts of materials and manufacturing methods must be considered. Optimum performance can be achieved by using a polishable glass with a gold or silver coating. There are many approaches to aligning a TMA, but a CMM, laser tracker, theodolite, and interferometer are tools that may be considered.

## Appendix – Table of Acronyms

Table 6: Acronyms

Acronym	Definition
CNC	Computer numerical control
CTE	Coefficient of thermal expansion
EPD	Entrance pupil diameter
FFOV	Full field of view
FOV	Field of view
HFOV	Half field of view
JWST	James Webb Space Telescope
MTF	Modulation transfer function
NA	Numerical aperture
RMSWFE	Root mean square wavefront error
SMR	Spherically mounted retroreflector
TMA	Three-mirror anastigmat
UUT	Unit under test

# References

- 
- <sup>1</sup> Raymond G. Marsh, H. Ned Sissel, "A Comparison Of Wide-Angle, Unobscured, All-Reflecting Optical Designs," Proc. SPIE 0818, Current Developments in Optical Engineering II, (1 January 1987).
- <sup>2</sup> Sasián, José. *Introduction to Aberrations in Optical Imaging Systems*. Cambridge, 2013.
- <sup>3</sup> Bentley, Julie, and Craig Olson. *Field Guide to Lens Design*. SPIE Press, 2012.
- <sup>4</sup> Hecht, Eugene, and Alfred Zajac. "5.7 Optical Systems." *Optics*, 4th ed., Addison-Wesley Publishing Company, 1974, pp. 138–159.
- <sup>5</sup> Andrew Rakich, "Reflecting anastigmatic optical systems: a retrospective," Opt. Eng. 57(10) 101701 (27 April 2018)
- <sup>6</sup> "New Horizons." NASA, NASA, Sept. 2023, [science.nasa.gov/mission/new-horizons](https://science.nasa.gov/mission/new-horizons).
- <sup>7</sup> Dennis Reuter, Alan Stern, James Baer, Lisa Hardaway, Donald Jennings, Stuart McMuldroy, Jeffrey Moore, Cathy Olkin, Robert Parizek, Derek Sabatke, John Scherrer, John Stone, Jeffrey Van Cleve, Leslie Young, "Ralph: a visible/infrared imager for the New Horizons Pluto/Kuiper belt mission," Proc. SPIE 5906, Astrobiology and Planetary Missions, 59061F (22 September 2005).
- <sup>8</sup> "JWST User Documentation." JWST Telescope - JWST User Documentation, Space Telescope Science Institute, 1 Dec. 2022, [jwst-docs.stsci.edu/jwst-observatory-hardware/jwst-telescope](https://jwst-docs.stsci.edu/jwst-observatory-hardware/jwst-telescope).
- <sup>9</sup> Greivenkamp, John E. *Field Guide to Geometrical Optics*. SPIE Optical Engineering Press, 2004.
- <sup>10</sup> Sasián, José. *Introduction to Lens Design*. Cambridge, 2019.
- <sup>11</sup> Carlino, Lawrence. "GSO 8-Inch True Cassegrain - Telescopes - Articles - Articles - Cloudy Nights." *Cloudy Nights*, 13 Dec. 2019, [www.cloudynights.com/articles/cat/user-reviews/telescopes/gso-8-inch-true-cassegrain-r3215](https://www.cloudynights.com/articles/cat/user-reviews/telescopes/gso-8-inch-true-cassegrain-r3215).
- <sup>12</sup> Fischer, Robert E., et al. "Design Forms." *Optical System Design*, 2nd ed., McGraw Hill, 2008, pp. 128–155.
- <sup>13</sup> Schott. ZERODUR - Extremely Low Expansion Glass Ceramic, Schott AG, Mainz, Germany, 2013.
- <sup>14</sup> Corning. Corning HPFS 7979, 7980, 8655 Fused Silica Optical Materials Product Information, Specialty Materials Division, Corning, NY, 2015.
- <sup>15</sup> Schott. BOROFLOAT33 - Mechanical Properties, Schott Technical Glass Solutions, Jena, Germany.
- <sup>16</sup> Schott. BOROFLOAT33 - Thermal Properties, Schott Technical Glass Solutions, Jena, Germany.
- <sup>17</sup> Datasheet: Schott N-BK7, Schott, 2023.
- <sup>18</sup> Soda-Lime Glass, Advanced Optics, Pewaukee, WI.
- <sup>19</sup> "6061 Aluminium Alloy." Wikipedia, Wikimedia Foundation, 7 Mar. 2024, [en.wikipedia.org/wiki/6061\\_aluminium\\_alloy](https://en.wikipedia.org/wiki/6061_aluminium_alloy).
- <sup>20</sup> Fountain, Glen H., et al. "The New Horizons Instrument Suite." Johns Hopkins APL Technical Digest (Applied Physics Laboratory) 37.1 (2023): 34-48.

- 
- <sup>21</sup> “Optical Coating.” Wikipedia, Wikimedia Foundation, 16 Oct. 2023, [en.wikipedia.org/wiki/Optical\\_coating](https://en.wikipedia.org/wiki/Optical_coating).
- <sup>22</sup> Rhorer, Richard L., and Chris J. Evans. “Chapter 41: Fabrication of Optics by Diamond Turning.” *Handbook of Optics*, McGraw-Hill, Columbus, OH, 2010.
- <sup>23</sup> “Fabrication.” *Coherent*, [www.coherent.com/optics/capabilities/fabrication](https://www.coherent.com/optics/capabilities/fabrication). Accessed 11 Apr. 2024.
- <sup>24</sup> *Superpolished Optics | Edmund Optics*, [www.edmundoptics.com/knowledge-center/trending-in-optics/superpolished-optics/](https://www.edmundoptics.com/knowledge-center/trending-in-optics/superpolished-optics/). Accessed 12 Apr. 2024.
- <sup>25</sup> “Polishing.” *Satisloh*, [www.satisloh.com/precision-optics/polishing](https://www.satisloh.com/precision-optics/polishing). Accessed 11 Apr. 2024.
- <sup>26</sup> Phillip Coulter, Raymond G. Ohl, Peter N. Blake, Brent J. Bos, Victor J. Chambers, William L. Eichhorn, Jeffrey S. Gum, Theodore J. Hadjimichael, John G. Hagopian, Joseph E. Hayden, Samuel E. Hetherington, David A. Kubalak, Kyle F. Mclean, Joseph C. McMann, Kevin W. Redman, Henry P. Sampler, Greg W. Wenzel, Jerrod L. Young, “A toolbox of metrology-based techniques for optical system alignment,” *Proc. SPIE 9951, Optical System Alignment, Tolerancing, and Verification X*, 995108 (20 October 2016)
- <sup>27</sup> “CMM (Coordinate Measuring Machine).” *KEYENCE*, 2024, [www.keyence.com/products/measure-sys/cmm/](https://www.keyence.com/products/measure-sys/cmm/).
- <sup>28</sup> “Understanding Laser Trackers.” *FARO.Com*, [www.faro.com/en/Resource-Library/Article/understanding-laser-trackers](https://www.faro.com/en/Resource-Library/Article/understanding-laser-trackers). Accessed 16 Apr. 2024.
- <sup>29</sup> “Leica TM6100A User Manual.” Leica Geosystems, 2009.
- <sup>30</sup> “Alignment Cubes - Precision Optics: Prisms: Custom Prisms: Precision Optical Inc..” *Precision Optics | Prisms | Custom Prisms | Precision Optical Inc.*, 23 June 2022, [www.precisionoptical.com/precision-optics/alignment-cube/](https://www.precisionoptical.com/precision-optics/alignment-cube/).
- <sup>31</sup> Goodwin, Eric P., and James C. Wyant. *Field Guide to Interferometric Optical Testing*. SPIE Press, 2006.
- <sup>32</sup> Conor W. Staples, Bob J. Brown, Brian C. Primeau, “TMA optical alignment using code V automatic design, code V alignment optimization, and Zernike sensitivity analysis,” *Proc. SPIE 11816, Optomechanics and Optical Alignment*, 1181608 (11 August 2021);